A low-cost approach to the skin effect compensation in cylindrical shunts

Marco Faifer, *Member, IEEE*, Roberto Ferrero, *Member, IEEE*, Christian Laurano, *Student Member, IEEE*, Roberto Ottoboni, *Fellow, IEEE*, Sergio Toscani, *Member, IEEE*, Michele Zanoni, *Student Member, IEEE*

***Abstract*—In this paper the development of a new design solution for high-current shunt resistors is presented, which allows achieving very good accuracy while requiring a simple and low-cost manufacturing process. It is based on a solid cylinder having the voltage measurement circuit which runs through two holes drilled in the cylinder itself. Starting from the well-known expression of the current density in a cylindrical conductor, the frequency response of the shunt is obtained in closed form as a function of the geometric parameters. In turn, the positions of the voltage measurement terminals are chosen by optimizing the frequency response function over a specified range. A shunt prototype has been manufactured and its measurement performance has been evaluated. The experimental results confirm the validity of the approach and highlight the significant improvement with respect to the single-hole cylindrical shunt which has been recently proposed by the authors. The obtained measurement accuracy is noticeable when compared with the ease of manufacturing.**

***Index Terms*— shunts; current measurement; skin effect; inductance; mutual coupling, frequency response, frequency-domain analysis, measurement techniques, calibration.**

I. Introduction

Current measurements can be performed by several methods, based on different physical principles, such as the Ohm's law, the Faraday-Lenz's law and the Hall effect, just to mention the main ones. Each method is characterized by its own peculiarities, in terms of current and frequency ranges, accuracy, thermal drift, power losses and electric insulation, which all contribute to determine the best solution for a particular application [1].

Shunt resistors are widely employed as current transducers because of their conceptual simplicity and their good accuracy over a wide range of both current amplitudes and frequencies. In particular, they are suited for measuring DC currents or those containing unidirectional components, for example because of transients or short circuits.

Nevertheless, some challenges arise when shunts are used for high current measurements. On the one hand, the need for a very low resistance because of thermal constraints also implies a very low inductance to maintain a large bandwidth, which is however difficult to obtain. On the other hand, the large cross-section required in high-current applications results in a strongly non-uniform current distribution at high frequencies because of skin effect, which in turn leads to an uneven frequency response of the shunt.

To overcome these issues, several design solutions have been proposed in the literature [2]-[5]. Among them, coaxial or cage shunt configurations have been proposed, together with a particular arrangement of the sensing wires in order to reduce the mutual coupling between the power and sense loops and to compensate (at least partially) for the skin effect.

A new approach based on a solid cylindrical shunt was employed by the authors in [6]. Basically, the voltage is collected within a hole drilled in the shunt itself. This choice allowed reducing size and simplifying the mathematical modeling, since the expression of the current distribution can be written in closed form. From a manufacturing point of view, the construction is considerably simpler than other solutions proposed in the literature [2], [3].

In this paper, an improvement of the aforementioned approach is proposed. The new shunt is provided with two holes, each of them accommodating one of the measurement terminals. The voltage measurement points are selected by optimizing the frequency response in a specified frequency range; the additional degree of freedom permits a significant improvement both in terms of bandwidth and overall accuracy with respect to the single-hole shunt.

In the next sections, the analytical model of the shunt already presented in [6] is briefly introduced and applied to the new measurement configuration. A prototype of the two-hole shunt has been manufactured and tested; its frequency response has been evaluated and compared both to that obtained with the single-hole configuration and to the analytical prediction. The experimental results confirm that the new measurement configuration allows a substantial performance improvement.

II. Analytical Model

Let us consider a solid, cylindrical conductor of radius r_0 made of a non-ferromagnetic material characterized by its resistivity ρ and magnetic permeability very close to μ_0. Introducing $I(j\omega)$ as the spectrum of the current flowing through the conductor, considering a length l where boundary effects can be neglected, the inner current density J in a point depends on r, namely its distance from the axis of the cylinder.

$$J\left(x, j\omega\right) = \frac{jkr_0}{2\pi r_0^2} \frac{J_0\left(jkr_0 x\right)}{J_1\left(jkr_0\right)} I\left(j\omega\right) \tag{1}$$

where J_0 and J_1 are first kind Bessel functions of order zero and one respectively; k and x are defined as:

$$k = \sqrt{\frac{j\omega\mu_0}{\rho}}\ ; \quad x = \frac{r}{r_0} \tag{2}$$

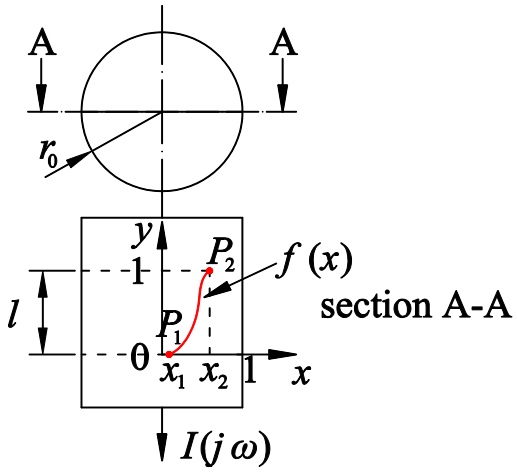

Fig. 1 Function $f(x)$ representing the voltage measurement path inside the shunt (red).

Now, let us suppose that this cylindrical conductor is employed as a shunt resistor for measuring the current I. It is clear that the choice of the voltage measurement path heavily affects the frequency response because of the uneven, frequency-dependent current distribution in the cross section as from (1). This phenomenon, known as skin effect, depends on the product kr_0. Thus, for a given material and frequency content of the current, it becomes stronger as r_0 is increased, namely when the shunt is designed to measure large currents.

The most straightforward choice is to collect the voltage across two points on the outer surface of the shunt, running the cables as close as possible in order to reduce the inductive coupling of the measurement circuit. However, it can be easily shown that the resulting frequency response is extremely poor; in fact, it has been known for a long time that better dynamic performance can be achieved if the measurement circuit is placed inside the shunt [2], [3].

In order to study the effect of the measurement path on the frequency response, the reference frame shown in Fig. 1 is introduced. Having considered the l-long part of the conductor, the dimensionless coordinate y is introduced, spanning between zero and one. Wire #1 electrically connects P_1 (x_1; y_1=0) to the negative input terminal of the voltmeter passing from P_2, whereas wire #2 connects point P_2 (x_2; y_2=1) to the positive input. Between P_2 and the voltmeter, the two wires follow the same path and are twisted so that the contribution to the flux linked with the measurement circuit is negligible.

Let us suppose that the path of wire #1 between P_1 and P_2 can be expressed by a generic curve represented by the function $y=f(x)$, which is shown in red in Fig. 1. The spectrum $V(j\omega)$ of the voltage signal collected by the voltmeter results:

$$V(j\omega)=\left[\rho_0 J(r_0 x_2, j\omega)-j\omega\Psi_{sp}(j\omega)\right]l \tag{3}$$

The specific magnetic flux density Ψ_{sp} per unit of length has been introduced; Ψ_{sp} can be computed starting from the spectrum of the flux density B inside the cylindrical shunt, which is given by:

$$B(x, j\omega)=\frac{\mu_0}{2\pi r_0}\frac{J_1(jkr_0 x)}{J_1(jkr_0)}I(j\omega) \tag{4}$$

Since the flux lines are circumferences concentric with the current-carrying conductor, Ψ_{sp} can be computed as:

$$\Psi_{sp}(j\omega)=r_0\int_{x_1}^{x_2}B(x, j\omega)\,f(x)\,dx \tag{5}$$

The frequency response function (FRF) $Z_s(j\omega)$ of the shunt is, by definition, the ratio between the spectrum of the output voltage and that of the current. Dividing it by its DC value, the normalized FRF $Z_{s,n}(j\omega)$ is obtained:

$$Z_{s,n}(j\omega)=\frac{jkr_0}{2J_1(jkr_0)}\left[J_0(jkr_0 x_2)+jkr_0\int_{x_1}^{x_2}J_1(jkr_0 x)\,f(x)\,dx\right] \tag{6}$$

The normalized FRF depends on the radius r_0 of the shunt and on the shape of the measurement circuit, hence on the function $f(x)$; the frequency-dependence is hidden in k. A previous paper [3] has shown that the choice $f(x)=x^2$, x_1=0, x_2=1 ideally results in a perfectly flat FRF, hence $Z_{s,n}(j\omega)$=1 regardless of the outer radius r_0. From a practical point of view, in this case the measurement circuit has to be inserted into the shunt by cutting it axially and machining a thin, parabolic groove to accommodate wire #1. Since this procedure is rather complex and expensive, it would be interesting to investigate the performance achieved with a much simpler solution: a straight measurement circuit [6]. In this case, the voltmetric terminals can be easily inserted by performing a thin hole in the shunt, thus drastically simplifying the manufacturing process. Let us consider the following measurement path $f(x)$:

$$f(x)=\frac{x-x_1}{x_2-x_1} \tag{7}$$

It corresponds to a measurement circuit which goes straight from the radial position $x_1 r_0$ to $x_2 r_0$ in the considered length l, as shown in Fig. 2.

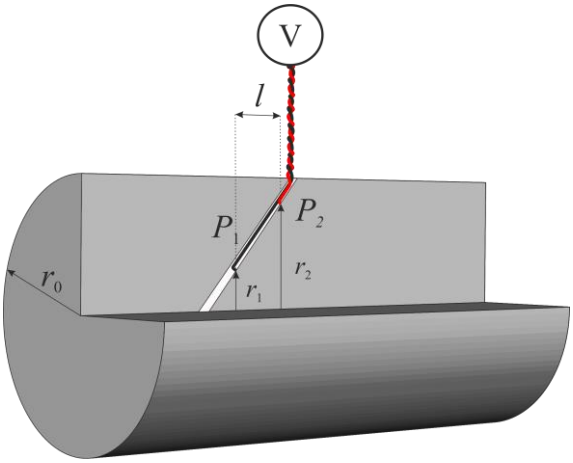

Fig. 2 Single-hole shunt and measurement circuit.

Substituting (7) into (6) and performing the integration by using some properties of the Bessel functions [7] allow obtaining the following analytical expression of the normalized FRF:

$$Z_{s,n}(j\omega)=\frac{jkr_0}{2kr_0(x_2-x_1)J_1(jkr_0)}\left\{\frac{1}{6}(kr_0)^3\left[x_1^3\,{}_1F_2\left(\frac{3}{2};2,\frac{5}{2};\frac{(kr_0x_1)^2}{4}\right)+\right.\right.$$
$$\left.\left.-x_2^3\,{}_1F_2\left(\frac{3}{2};2,\frac{5}{2};\frac{(kr_0x_2)^2}{4}\right)\right]+kr_0\left[x_2J_0(jkr_0x_2)-x_1J_0(jkr_0x_1)\right]\right\} \tag{8}$$

${}_1F_2$ denotes the generalized hypergeometric function having one type-1 parameter and two type-2 parameters.

From (8) it can be noted that the normalized FRF does not

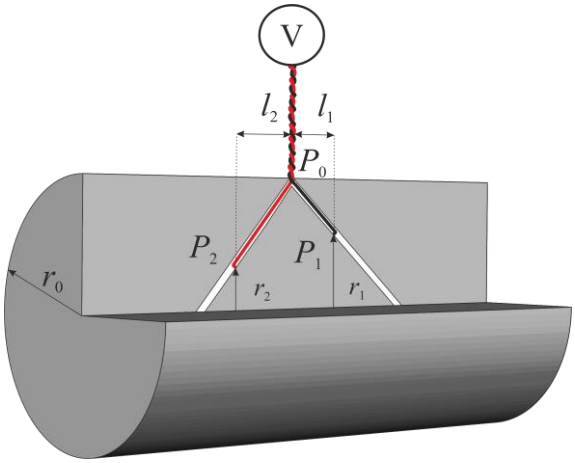

Fig. 3 Two-hole shunt and measurement circuit.

depend on the slope of the measurement path, but only on the radial positions of the two measurement points P_1 and P_2. Thus, the length l just affects the DC gain of the shunt frequency response.

A simple, straight measurement path allows obtaining good performance [6] in the frequency range 10 Hz – 1 kHz; however, better results can be achieved if a slightly more complex configuration is employed. Therefore, let us consider the measurement circuit shown in Fig. 3. The cylindrical shunt is now provided with two holes forming the same angle with respect to the outer surface; each of them accommodates one of the voltmetric wires. Wire #1 connects the negative terminal of the voltmeter to P_1, characterized by its radial coordinate r_1 (x_1 in per units); similarly, wire #2 runs from the positive terminal of the voltmeter to P_2, having radial coordinate r_2 (x_2 in per units). In P_0 the two wires exit from the shunt and are twisted so that the contribution to the flux linkage due to the magnetic field outside the shunt is negligible. l_1 represents the axial distance between P_1 and P_0, whereas l_2 is the axial distance between P_2 and P_0. The spectrum $V(j\omega)$ of the measured voltage can be decomposed into the sum of two contributions:

$$V(j\omega) = V_1(j\omega) + V_2(j\omega) \tag{9}$$

The first one corresponds to the voltage measured by a voltmeter whose positive terminal is connected to the point P_0 on the outer surface of the shunt, whereas the negative one is connected to wire #1, having assumed that the flux linkage due to the field outside the shunt is zero. The second contribution represents the voltage read by another voltmeter having the positive terminal connected to P_0 and the negative one to wire #2 under the same assumptions. It should be noticed that in this way the study of the two-hole shunt can be performed by using the expressions previously obtained for the single-hole shunt. In particular $Z_{s1,n}(j\omega)$ and $Z_{s2,n}(j\omega)$, namely the normalized FRFs of the two voltage contributions to the current flowing through the shunt can be obtained by using (8). After some simple computations, the analytical expression of the normalized FRF $Z_{d,n}(j\omega)$ of the two-hole shunt comes straightforwardly:

$$Z_{d,n}(j\omega) = \frac{Z_{s1,n}(j\omega)l_1 + Z_{s2,n}(j\omega)l_2}{l_1 + l_2} \tag{10}$$

It is the weighted average between $Z_{s1,n}(j\omega)$ and $Z_{s2,n}(j\omega)$

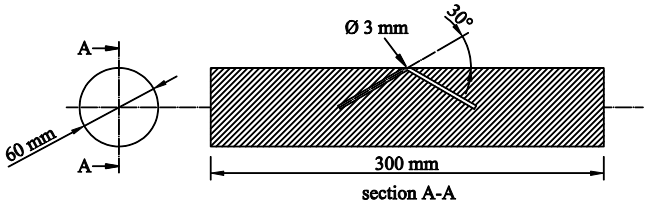

Fig. 4 Characteristic dimensions of the two-hole shunt prototype.

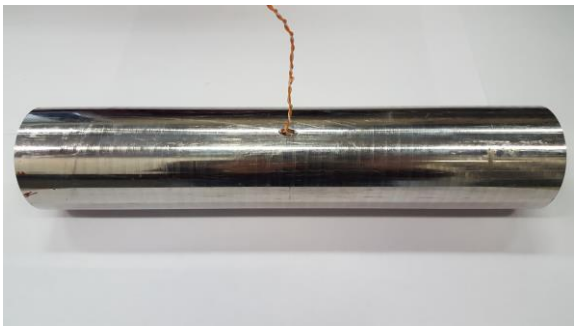

Fig. 5 Photograph of the shunt prototype.

where the weights are represented by l_1 and l_2, respectively. It can be rewritten as:

$$Z_{d,n}(j\omega) = \frac{(1-x_1)Z_{s1,n}(j\omega) + (1-x_2)Z_{s2,n}(j\omega)}{2 - x_1 - x_2} \tag{11}$$

The normalized frequency response functions $Z_{s,n}(j\omega)$ and $Z_{d,n}(j\omega)$ of the single-hole and two-hole shunt synthesize the respective dynamic performances; for a given outer radius r_0 they depend on the measurement positions x_1 and x_2. Therefore, it is interesting to study which positions optimize the measurement performance over a predetermined frequency range. In order to quantify the accuracy, the Total Vector Error (TVE) is introduced. For each frequency component of the current, it corresponds to the distance on the complex plane between its actual phasor and that obtained from the shunt voltage, assuming that it has a perfectly flat response characterized by its DC resistance value. It is usually expressed as a percentage of the actual current, thus resulting:

$$TVE(j\omega) = \left|1 - Z_n(j\omega)\right| \tag{12}$$

where $Z_n(j\omega)$ is equal to $Z_{s,n}(j\omega)$ or $Z_{d,n}(j\omega)$ for the single-hole and two-hole shunt, respectively.

III. Single-hole and two-hole prototypes

The prototypes of the two proposed shunts have been built starting from a cylinder made of AISI 304, austenitic stainless steel. The outer radius r_0 is equal to 30 mm and the overall length is 300 mm; the material resistivity has been preliminarily tested, resulting to be $7.47 \cdot 10^{-7}$ Ωm at 20°C ambient temperature. A hole having a 3 mm diameter has been drilled in order to accommodate the measurement circuit; it is angled by 30° with respect to the outer surface, and its axis is coplanar with that of the shunt. Hole diameter should be as small as possible in order to minimize its effect on the current distribution, thus resulting in a better agreement between numerical simulations and experimental results. The two-hole shunt prototype has been obtained by

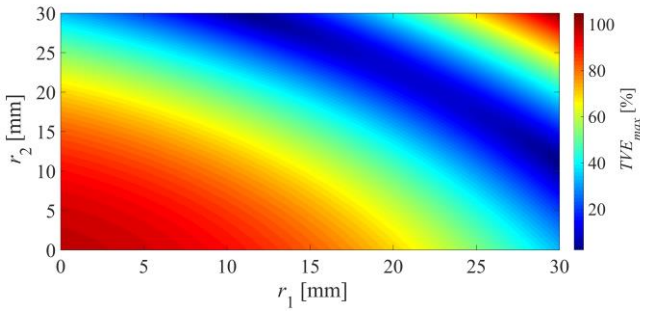

Fig. 6 Maximum TVE as function of the radial positions of the measurement terminals: single-hole shunt, DC-1 kHz frequency range.

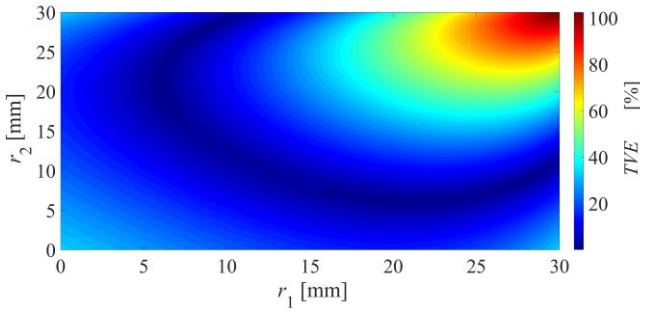

Fig. 7 Maximum TVE as function of the radial positions of the measurement terminals: two-hole shunt, DC-1 kHz frequency range.

drilling another 3 mm hole as depicted in Fig. 4. A photograph of the prototype is shown in Fig. 5

Having selected a frequency range, by using the models presented in the previous section, it is possible to predict the normalized FRF and the TVE for given radial positions r_1 and r_2 of P_1 and P_2 respectively. The investigated frequency range strictly depends on the peculiar application; the frequency range DC-1 kHz has been considered at first.

The maximum TVE has been computed in this range for both the single-hole and two-hole shunt. The results, reported in Fig. 6 and Fig. 7, highlight the strong dependency of the performance on the measurement path, and allow locating the optimal measurement points.

When the single-hole shunt is considered, the best performance is achieved for r_1=10.8 mm, r_2=r_0 (x_1=0.18, x_2=1) corresponding to a voltmetric terminal inserted into the hole, and the other one placed on the outer surface of the shunt. This choice results in a maximum TVE of 2.5%. The predicted performance of the two-hole shunt is considerably better, since the TVE is 0.11% when r_1=21 mm, r_2=6 mm (x_1= 0.7, x_2 = 0.2). Fig. 8 compares the predicted TVEs for the two solutions, optimized for the frequency range DC-1 kHz. Conversely, it is interesting to notice that if the voltage is collected on the cylinder surface, the predicted maximum TVE exceeds 104%.

Because of the remarkable performance achieved by the two-hole solution, it is interesting to find the measurement positions which minimize the TVE over a broader bandwidth, such as DC-5 kHz. As for the previous frequency range, an optimization process has been performed for both the single-hole and the two-hole shunts in order to find the voltage measurement positions resulting in the lowest maximum TVE. Considering the best

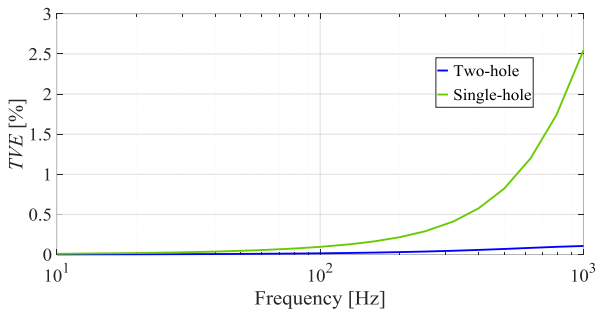

Fig. 8 TVE of the single-hole and two-hole shunt: performance optimized in the range DC-1 kHz.

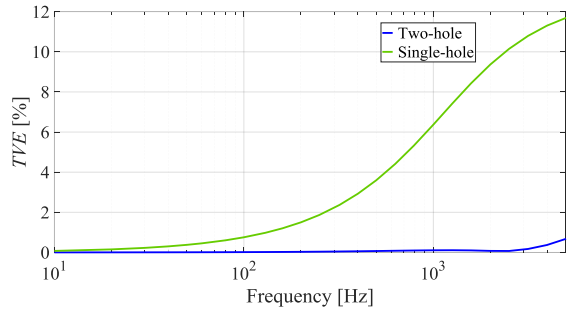

Fig. 9 TVE of the single-hole and two-hole shunt: performance optimized in the range DC-5 kHz.

measurement positions, the TVE versus frequency plot obtained for the single-hole and two-hole shunts are compared in Fig. 9. Having extended the frequency range, the TVE of the single hole shunt increases dramatically, reaching almost 12% at 5 kHz. It should be noticed that even the TVE at 1 kHz is considerably higher, being now above 6%. The reason is that the radial positions returned by the new optimization are different, being now r_1=12.6 mm, r_2=30 mm. The new, two-hole solution reaches better accuracy, with a maximum TVE equal to 0.68% at 5 kHz, a remarkable result if compared to the simple construction. Furthermore, it should be noticed that in this case minimizing the TVE in the range DC-1 kHz returns the same radial position as considering the broader frequency range DC-5 kHz.

A shunt is a linear time invariant (LTI), single-input single-output system. As from (12), its performance can be assessed by injecting a test current and measuring the FRF over the frequency range of interest. It should be noticed that this characterization requires a proper generator with adequate current capability in the frequency range of interest. The test signal amplitude is fundamental in order to obtain a good Signal to Noise Ratio (SNR), hence a low measurement uncertainty. In this respect, the shunt prototypes have been manufactured using AISI 304 stainless steel because of its paramagnetic behavior and fairly high resistivity which allows reducing the test current. On the other hand, a large current may heat the material and therefore change its resistivity and the response of the shunt. Hence, as for any high-precision shunt resistor, an alloy having a resistivity that weakly depends on temperature (i.e. manganin) is recommended for practical applications.

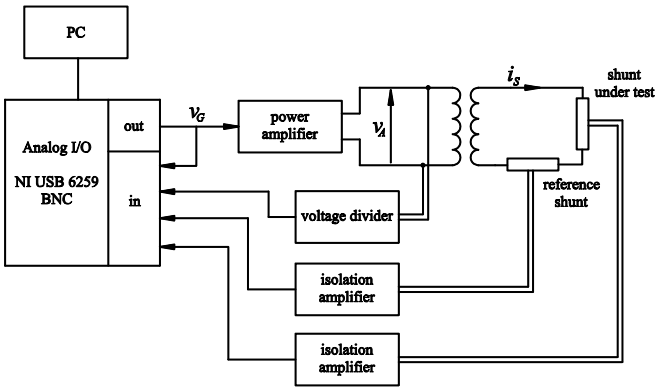

Fig. 10 Architecture of the experimental setup.

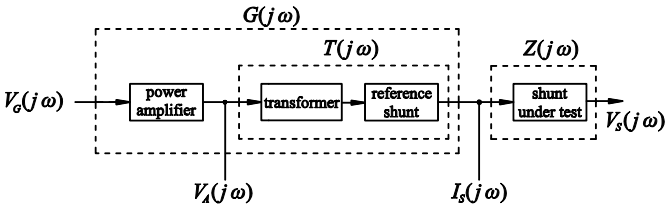

Fig. 11 Block diagram of the current generator.

IV. Experimental Setup

The shunt prototypes have been tested by using a custom current generator. Its architecture resembled that of a voltage generator [8], [9] previously developed by the authors for testing of medium voltage transducers; the architecture is shown in Fig. 10. Basically, it consists of a signal generator connected to a power amplifier (whose specifications are summarized in TABLE I.) that feeds a step-down transformer having a 100:5 turn ratio, thus boosting the output current. The high-current winding of the transformer has been connected to the shunt under test and to a reference current transducer, namely a class 0.5 coaxial shunt characterized by DC-20 kHz frequency range and 100 A rated current. Because of the low ohmic resistance of the shunts, the output voltages are rather low even when fairly high currents are injected. For this reason, two Analog Devices AD215BY isolation amplifiers in noninverting configuration with a nominal gain of 100 have been employed. Their gains have been evaluated, and after calibration the residual gain error is lower than 100 ppm in the range DC-5 kHz. A wide bandwidth voltage probe has been employed to measure the power amplifier output voltage.

The input signal of the power amplifier has been provided by an analog output channel of a National Instrument NI USB-6259 board, which has been also employed to sample the amplifier output voltage and the output signals of the two shunts. The board is characterized by a maximum aggregate sampling rate of 1 Msamples/s, 16 bit resolution and ±10 V range. Signal generation and data acquisition have been managed by a PC, which has also performed the required signal processing; a sampling rate of 100 kHz has been chosen. The data acquisition device is characterized by a multiplexed architecture; therefore, for higher measurement accuracy, the interchannel delays have been estimated and compensated in the frequency domain.

TABLE I. Power Amplifier Specifications

Maximum output voltage	140 V
Voltage gain	From -∞ to 34 dB
-3dB bandwidth	5 Hz-50 kHz
SNR	>100 dB

Ensuring that the power amplifier and the transformer operate below saturation, the whole system can be considered as LTI with good accuracy, so that it can be represented by the block diagram reported in Fig. 11. Hence, after having estimated the FRF $G(j\omega)$, it is possible to compute the spectrum of the signal generator output voltage $V_G(j\omega)$ which allows obtaining the desired test current, characterized by the spectrum $I_{s,ref}(j\omega)$. The FRF $T(j\omega)$ allows predicting whether $I_{s,ref}(j\omega)$ is compatible with the maximum voltage output of the amplifier and the maximum magnetic flux of the transformer. Having injected the test current in the shunt, it is easy to compute its FRF $Z(j\omega)$, which represents the target of the characterization.

V. Experimental Results

In order to evaluate the dynamic performance of the two shunts, the experiment setup described in the previous section has been employed. First of all, $G(j\omega)$ over the frequency range between f_{min}=10 Hz and f_{max}=1 kHz has been measured. A quasi-logarithmic multisine signal with random phases and amplitude compensation [10] has been applied to the power amplifier and 200 periods of the consequent signals have been acquired. The spectral content is particularly suitable for system identification over a wide frequency range, since it allows attaining the same uncertainty over the whole range. $I_S(j\omega)$ is the spectrum of the current measured by the reference shunt averaged over the 200 acquired periods. Introducing $V_G(j\omega)$ as the spectrum of the generated voltage, $G(j\omega)$ can be estimated as:

$$G(j\omega) = \frac{I_S(j\omega)}{V_G(j\omega)} \tag{13}$$

The FRF $T(j\omega)$ has been measured by following the same approach. After that, the generator has been employed to inject a quasi-logarithmic, random phase multisine test current with frequency content between f_{min} and f_{max}; its peak and rms amplitudes were about 30 A and 9 A respectively, so that shunt self-heating is totally negligible. Under these conditions, the TVE of the generated current has been evaluated as lower than 0.1%, hence comparable with the uncertainty of the reference transducer. The voltage outputs of the two shunts have been acquired for M=200 periods. The spectrum $I_s(j\omega)$ of the current measured by the reference shunt and its sample standard deviation $s_{Is}(j\omega)$ can be easily computed starting from the 200 acquired periods by using the well-known expressions; the relative standard deviation estimates the signal to noise ratio, and it resulted to be lower than -80 dB. In the same way, the average spectrum $V_S(j\omega)$ of the shunt under test output as well as its sample standard deviation $s_{Vs}(j\omega)$ have been obtained; the relative value of the latter is below -60 dB over the whole frequency range. The FRF $Z(j\omega)$ of the shunt under test has been estimated as:

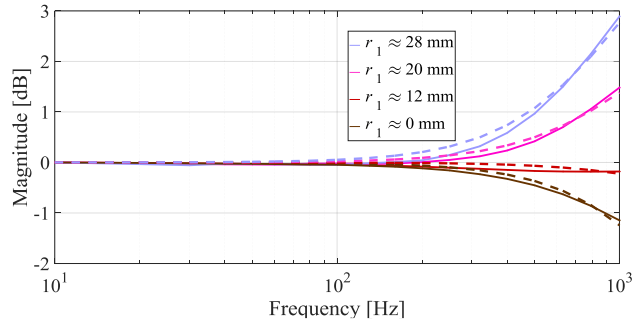

Fig. 12 Magnitude response of the single-hole shunt for different voltage measurement positions, DC-1 kHz frequency range.

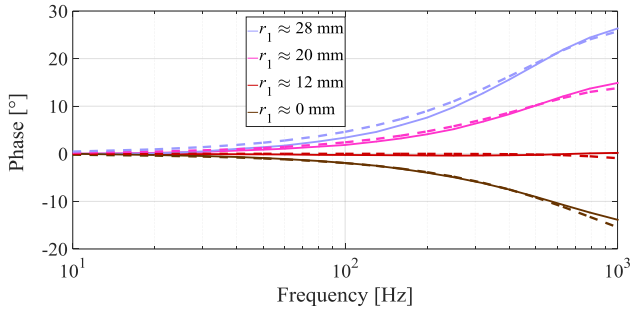

Fig. 13 Phase response of the single-hole shunt for different voltage measurement positions, DC-1 kHz frequency range.

$$Z(j\omega) = \frac{V_S(j\omega)}{I_S(j\omega)} \tag{14}$$

Having computed the sample covariance $s^2_{VsIs}(j\omega)$ between the two spectra, the standard deviation of $Z(j\omega)$ is obtained as [11]:

$$s_Z(j\omega) \approx \frac{|Z(j\omega)|}{\sqrt{M}} \sqrt{\frac{s^2_{V_S}(j\omega)}{|V_S(j\omega k)|^2} + \frac{s^2_{I_S}(j\omega)}{|I_S(j\omega k)|^2} - 2\Re\left(\frac{s^2_{V_S I_S}(j\omega)}{V_S(j\omega) I^*_S(j\omega)}\right)} \tag{15}$$

First of all, the single-hole shunt has been considered; its FRF in the range DC-1 kHz has been evaluated for different voltage measurement positions. The voltmetric terminal #2 has been pressed on the outer surface of the shunt, as close as possible to the hole. The other wire #1 has been inserted into the hole so that its bare end touches the inner surface. The length of wire inserted into the hole has been changed, so that the FRFs for different values of the radial position r_1 have been estimated. Some results are reported in Fig. 12 and Fig. 13 (continuous lines) and compared with those predicted by the model (dotted lines). Unfortunately, the test setup does not allow an accurate control of the radial position of the terminal #1; this is responsible for most of the differences between theoretical and measured frequency responses. In addition, the analytical model does not take into account the effect of the hole on the current distribution. Finally, since this hole is larger than the measurement wire, the measurement path may be not exactly a straight line.

The target of the experimental activity is to find the optimal measurement position that minimizes the TVE of the shunt in the range DC-1 kHz. The TVE has been evaluated for each FRF, the best one has been compared with the analytical prediction as shown in Fig. 14 (green lines); it corresponds to the red continuous traces reported in Fig. 12 and Fig. 13. Because of the small values, results are extremely sensitive to unmodeled effects. For low

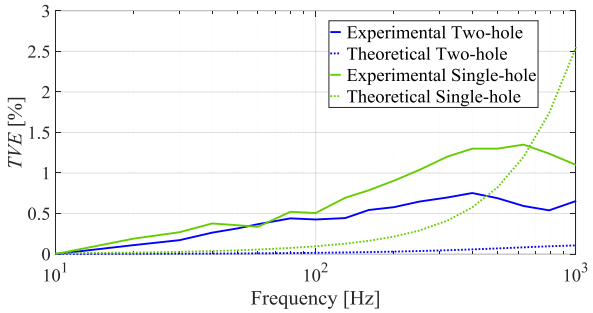

Fig. 14 TVEs of the two shunts (analytical predicion and experimental results) DC-1 kHz frequency range.

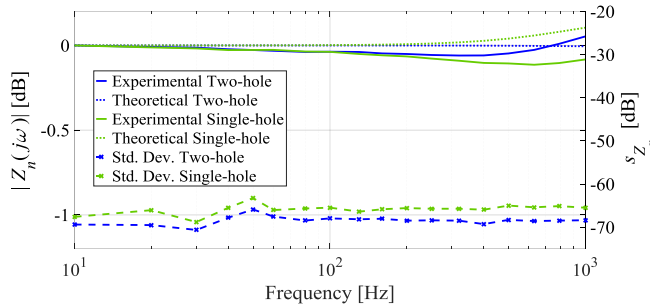

Fig. 15 Magnitude responses of the two shunts (analytical prediction and experimental results) DC-1 kHz frequency range.

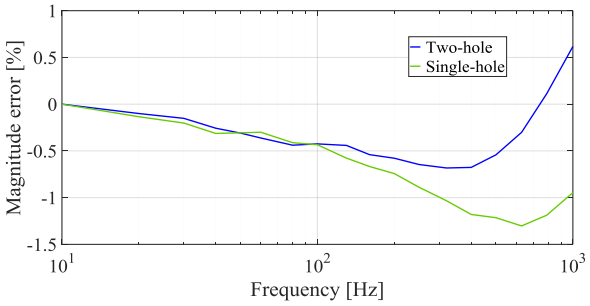

Fig. 16 Magnitude errors of the two shunts, DC-1 kHz frequency range.

frequencies, the experimental TVE is higher than the theoretical one since the roll-off of the measured FRF begins earlier. On the contrary, at higher frequencies the measured TVE is lower than that computed with the analytical model. This is essentially due to the experimental phase response, which is considerably flatter than the prediction [6]. The best measurement point resulted in a maximum TVE of 1.35%, therefore slightly lower than the 2.32% predicted by the model. When looking at the magnitude error reported in Fig. 16 (green trace) it can be noticed that the maximum TVE is essentially due to the magnitude response of the shunt.

After that, the two-hole shunt has been tested. The current generator has been employed to evaluate the FRFs in the range DC-1 kHz obtained by changing the measurement positions r_1 and r_2. For each of them, the TVE has been computed, and the frequency response obtained in the best measurement position has been compared with the analytical prediction and with that obtained with the single-hole configuration. The comparison between the TVEs is reported in Fig. 14. The maximum TVE is now equal to 0.75%, therefore nearly half of that reached by the single-hole configuration, even if considerably higher than the

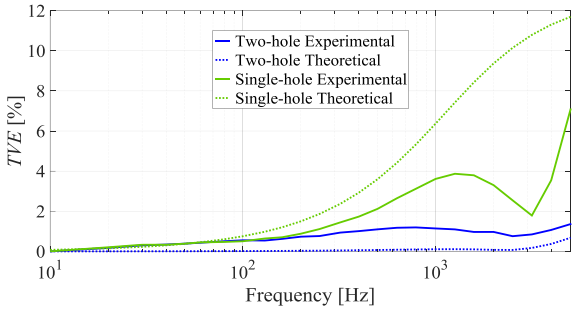

Fig. 17 TVEs of the two shunts (analytical predicion and experimental results) DC-5 kHz frequency range.

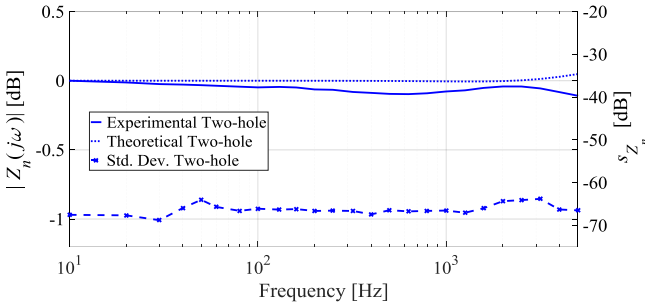

Fig. 18 Magnitude response of the two-hole shunt (analytical prediction and experimental results) DC-5 kHz frequency range.

theoretical prediction. In this case, being the theoretical skin effect compensation more effective than in the single-hole shunt, parasitic phenomena and mechanical tolerances have now a greater impact on the experimental results.

For the sake of completeness, the normalized magnitude response obtained for the two-hole shunt is reported in Fig. 15 (blue lines) together with that of the single-hole shunt and the analytical predictions. Fig. 18Fig. 16 shows also the magnitude error of the two-hole shunt (blue line). By comparing it to Fig. 14, also in this case it can be noticed that the maximum TVE is almost totally due to the magnitude response of the shunt.

Having proven the best accuracy of the two-hole configuration, it is now interesting to investigate its performance over a broader frequency range. Therefore, the same procedure performed for the previous test has been carried out by increasing the frequency limit up to f_{max} = 5 kHz. The best measurement positions have been found both for the single-hole and the two-hole shunts. The obtained TVEs are compared in Fig. 17. The TVE achieved by the two-hole configuration is lower than 1.36%, which is a remarkable result when compared with its simple, low-cost construction, albeit substantially higher than the analytical prediction (0.68 %). Experimental results confirm that the single-hole shunt is not suitable for accurate measurements above 1 kHz, since the maximum TVE reaches about 7%, in this case considerably lower than the value predicted by the analytical model. In any case, as stated before, an accurate performance prediction is extremely hard to be achieved because of the small values of the errors. Therefore, model approximations and uncertainties may have a dramatic impact on the predicted TVE values.

The normalized magnitude response of the two-hole shunt optimized for the DC-5 kHz frequency range is reported in Fig. 18, which shows a very flat behavior. However, for

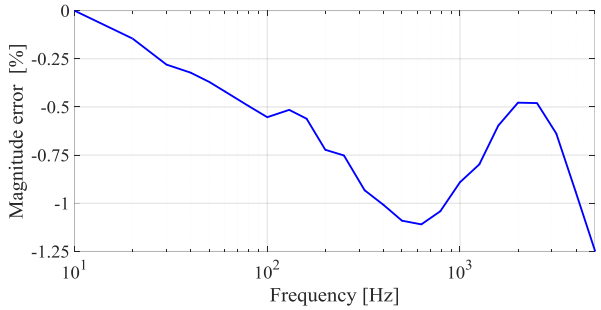

Fig. 19 Two-hole shunt magnitude error.

frequencies of some hundreds of hertz, the experimental response contains a small dip, which is not predicted by the analytical model. Furthermore, experimental results show a slight attenuation in the right part of the spectrum, whereas the contrary is expected from the model. Both of these effects have a visible impact in the magnitude error of the two-hole shunt, which is shown in Fig. 19. It should be noted that the maximum magnitude error is 1.25% at 5 kHz, which is just slightly lower than the maximum TVE. This means that the phase shift introduced by the shunt has an almost negligible impact. In fact, when looking at the phase error plot the maximum value is about 0.4°, hence rather small.

VI. Conclusion

In this paper, a simple, low-cost solution to compensate for skin effect in cylindrical shunts has been proposed. The expedient consists in collecting the voltage inside the shunt by means of one or two holes which can be easily obtained by drilling. The analytical expression of the shunt frequency response has been obtained; it helps choose the positions of the voltage measurement terminals in order to optimize the performance over a predetermined frequency range. The model shows that good accuracy can be achieved with the single-hole shunt in the frequency range DC-1 kHz. Considerably better performance is expected from the two-hole configuration, since the frequency range can be extended to 5 kHz without sacrificing the accuracy.

The proposed approach has been experimentally tested, and the results have shown a good agreement with the analytical predictions if the model approximations and the uncertain position of the measurement circuit are taken into account. The two-hole shunt achieved a TVE below 0.75% in the frequency range DC-1 kHz, half with respect to the single-hole configuration (1.35%). When the frequency range is extended up to 5 kHz, the TVE reaches 1.36%. Hence, the two-hole shunt has the same accuracy as the single-hole one, but achieved in a frequency range which is five times broader. Therefore, the proposed two-hole shunt prototype allows reaching remarkable performance, especially when considering the large cross sectional area and the simple construction.

References

[1] S. Ziegler, R. C. Woodward, H. H.-C. Iu, and L. J. Borle, "Current sensing techniques: A review," *IEEE Sensors J.*, vol. 9, no. 4, pp. 354–376, Apr. 2009.

[2] C. T. Nguyen and R. Malewski, "A novel principle of distortionless measurement of current impulse," *Proc. IEEE*, vol. 69, no. 4, pp. 490–491, Apr. 1981.

[3] R. Malewski, C. T. Nguyen, K. Feser, and N. Hylten-Cavallius, "Elimination of the skin effect error in heavy-current shunts," *IEEE*

Trans. Power App. Syst., vol. PAS-100, no. 3, pp. 1333–1340, March 1981.

[4] C. M. Johnson and P. R. Palmer, "Current measurement using compensated coaxial shunts," *Proc. Inst. Elect. Eng.—Sci. Meas. Technol.*,vol. 141, no. 6, pp. 471–480, Nov. 1994.

[5] R. Ferrero, M. Marracci, and B. Tellini, "Analytical study of impulse current measuring shunts with cage configuration," *IEEE Trans. Instrum. Meas.*, vol. 61, no. 5, pp. 1260-1267, May 2012.

[6] M. Faifer, C. Laurano, R. Ottoboni, S. Toscani, M. Zanoni, R. Ferrero, "Simple skin effect compensation in cylindrical shunts", in *Proc. IEEE Int. Workshop on Applied Measurements for Power Systems*, Aachen, Germany, Sept. 2016, pp. 155-160

[7] W. Rosenheinrich, "Tables of some indefinite integrals of Bessel functions, " Accessed on: May 2016 [Online]. Available: www.eah-jena.de/~rsh/Forschung/Stoer/besint.pdf.

[8] M. Faifer, R. Ottoboni, S. Toscani, C. Cerbaucich, M. Gentili, P. Mazza, "A medium voltage signal generator for the testing of voltage measurement transducers", *Proc. IEEE Instrum. Meas. Technol. Conf.*, 2013, pp. 194-199.

[9] M. Faifer, R. Ottoboni, S. Toscani, P. Mazza, C. Cerbaucich. "Metrological characterization of a signal generator for the testing of medium voltage measurement transducers", *IEEE Trans. Instrum. Meas.*, vol. 64, no. 7 , pp. 1837-1846, July 2015.

[10] E. Geerardyn, Y. Rolain, J. Schoukens, "Design of quasi-logarithmic multisine excitations for robust broad frequency band measurements", *IEEE Trans. Instrum. Meas.*, vol. 62, no. 5, pp. 1364-1372, 2013.

[11] R. Pintelon and J. Schoukens. "System identification: a frequency domain approach", 2nd Ed., Boston: Wiley & Sons, 2012.